

Medicinal Chemistry

Organometallic Derivatization of the Nematocidal Drug Monepantel Leads to Promising Antiparasitic Drug Candidates

Jeannine Hess,^[a] Malay Patra,^[a] Loganathan Rangasamy,^[a] Sandro Konatschnig,^[a] Olivier Blacque,^[a] Abdul Jabbar,^[b] Patrick Mac,^[c] Erik M. Jorgensen,^[c] Robin B. Gasser,^{*[b]} and Gilles Gasser^{*[a]}

Abstract: The discovery of novel drugs against animal parasites is in high demand due to drug-resistance problems encountered around the world. Herein, the synthesis and characterization of 27 organic and organometallic derivatives of the recently launched nematocidal drug monepantel (Zolvix[®]) are described. The compounds were isolated as racemates and were characterized by ¹H, ¹³C, and ¹⁹F NMR spectroscopy, mass spectrometry, and IR spectroscopy, and their purity was verified by microanalysis. The molecular structures of nine compounds were confirmed by X-ray crystallography. The anthelmintic activity of the newly designed

analogues was evaluated in vitro against the economically important parasites *Haemonchus contortus* and *Trichostrongylus colubriformis*. Moderate nematocidal activity was observed for nine of the 27 compounds. Three compounds were confirmed as potentiators of a known monepantel target, the ACR-23 ion channel. Production of reactive oxygen species may confer secondary activity to the organometallic analogues. Two compounds, namely, an organic precursor (**3a**) and a cymantrene analogue (**9a**), showed activities against microfilariae of *Dirofilaria immitis* in the low microgram per milliliter range.

Introduction

Multicellular parasites, including roundworms (nematodes), flatworms (trematodes and cestodes), and arthropods (e.g., fleas, flies, and ticks), cause morbidity and mortality in animals worldwide,^[1] which result in a substantial loss to global food production annually.^[1b,g] The control of parasites relies largely on the use of antiparasitic drugs.^[2] However, drug resistance is

now quite widespread.^[1a,3] Therefore, the development of new drugs or chemical modification of existing drugs is crucial to ensure sustainable chemical control of parasites in the future.

In this context, the discovery of the structurally new amino-acetonitrile class of synthetic antiparasitic compounds (AADs, see Figure 1) by Novartis Animal Health was a major breakthrough in 2008.^[4] An extensive structure–activity relationship (SAR) study resulted in the development of monepantel (AAD 1566, Figure 1), which was released under the trade name Zolvix[®] in 2009 for the treatment of nematode infections in sheep.^[5]

[a] J. Hess, Dr. M. Patra, Dr. L. Rangasamy, S. Konatschnig, Dr. O. Blacque, Prof. Dr. G. Gasser
Department of Chemistry, University of Zurich
Winterthurerstrasse 190, 8057 Zurich (Switzerland)
E-mail: gilles.gasser@chem.uzh.ch

[b] Dr. A. Jabbar, Prof. Dr. R. B. Gasser
Faculty of Veterinary and Agricultural Sciences
The University of Melbourne
Parkville, Victoria 3010 (Australia)
E-mail: robinbg@unimelb.edu.au

[c] P. Mac, Dr. E. M. Jorgensen
Howard Hughes Medical Institute
Department of Biology, University of Utah
Salt Lake City, UT 84112-0840 (USA)

Supporting information and ORCID number from the author for this article are available on the WWW under <http://dx.doi.org/10.1002/chem.201602851>.

It contains general remarks (materials, instrumentation and methods, X-ray crystallography, cell culture, cytotoxicity studies, ROS generation, biological assays, electrophysiology methods), synthesis and characterization of **3a–3n**, **5b–5k**, **7a**, **7b**, **8c**, **9a**, **9b**, NMR spectra, molecular structures of **3a**, **3b**, **3g**, **5a**, **5c**, **5h**, and **5k**, crystal data and structure refinement for **3a**, **3b**, **3f**, **3g**, **5a**, **5c**, **5d**, **5h**, and **5k**, antiparasitic activity against *C. felis*, *L. cuprina*, and *R. sanguineus* of organometallic derivatives **3a–3n**, **5a–5k**, **7a**, **7b**, **9a**, and **9b**, and ¹H NMR spectra of **3a** and **9a** at different time intervals.

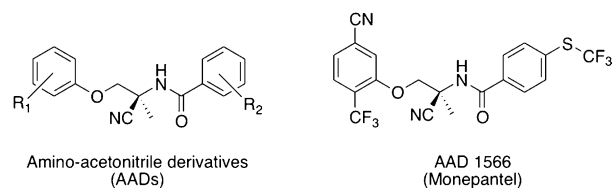


Figure 1. General structure of amino-acetonitrile derivatives (AADs) and monepantel (AAD 1566).

Monepantel targets ligand-gated ion channels in the nematode-specific DEG-3 family.^[4] These channels are related to nicotinic acetylcholine receptors, but they are gated by betaine and choline rather than acetylcholine.^[6] Monepantel acts on MPTL-1 receptors in *Haemonchus contortus* and the homologues ACR-20 and ACR-23 in the free-living nematode *Caenorhabditis elegans*. The drug acts as a positive allosteric modula-

tor, hyperactivating these channels.^[6c,7] An in vitro selection procedure by Rufener et al. revealed that monepantel resistance in *H. contortus* can develop relatively rapidly by a single loss-of-function mutation. Indeed, monepantel-resistant worms in livestock were reported within a few years.^[3d,e,8]

It is of increasing importance to search for structurally or functionally unique classes of compounds to control parasites.^[3a] To date, this quest has been focused mainly on organic compounds, but metal-based compounds have had an impressive success in other fields of medicinal chemistry.^[9] Specifically, recent efforts have identified anticancer,^[10] antimalarial,^[11] anti-trypanosomal,^[12] antibacterial,^[13] and antischistosomal^[14] compounds. Organometallic complexes (i.e., compounds with at least one direct metal–carbon bond) are a class of metal compounds that have shown promise as anti-infectives.^[13,15] Ferroquine, the ferrocenyl analogue of the antimalarial drug chloroquine, is the most prominent example of an organometallic drug candidate used against parasites. The introduction of a ferrocenyl moiety alters the mode of action of the parent drug and renders it active against chloroquine-resistant *Plasmodium falciparum* strains.^[11a] Similarly, an altered mode of action was evident in the ferrocenyl derivative of the anticancer drug tamoxifen, named ferrocifen. Whereas tamoxifen is only active against estrogen-positive breast cancers, ferrocifen is active against both estrogen-negative and estrogen-positive cancers.^[16] To the best of our knowledge, organometallic complexes have rarely been tested for nematocidal activity.^[17]

With the aim of developing new classes of nematocidal drugs, we recently initiated a program to design and test organometallic analogues of the organic anthelmintic monepantel. The aryloxy unit of the original molecule was substituted with sandwich (ferrocene, ruthenocene) and half-sandwich (cymantrene) organometallic moieties in order to introduce metal-specific modes of action, as well as with various organic moieties. The functional groups at the benzamide unit of the organometallic and organic analogue were further varied (SCF₃, OCF₃, CF₃, F, Cl, Br, I, etc.). The presence of different functional groups is expected to modulate the lipophilicity, biodistribution, and pharmacokinetic properties, thereby influencing the biological properties of the newly designed monepantel analogues. These modifications resulted in a library of 27 organic/organometallic derivatives of monepantel for SAR studies. The initial biological screenings reported herein demonstrate that some of the compounds retain activity against monepantel targets, while gaining novel properties such as the production of reactive oxidative species (ROS). Additionally, we demonstrate for the first time that AADs, including our organic and organometallic analogues, show activity against *Diriofilaria immitis* microfilariae.

Results and Discussion

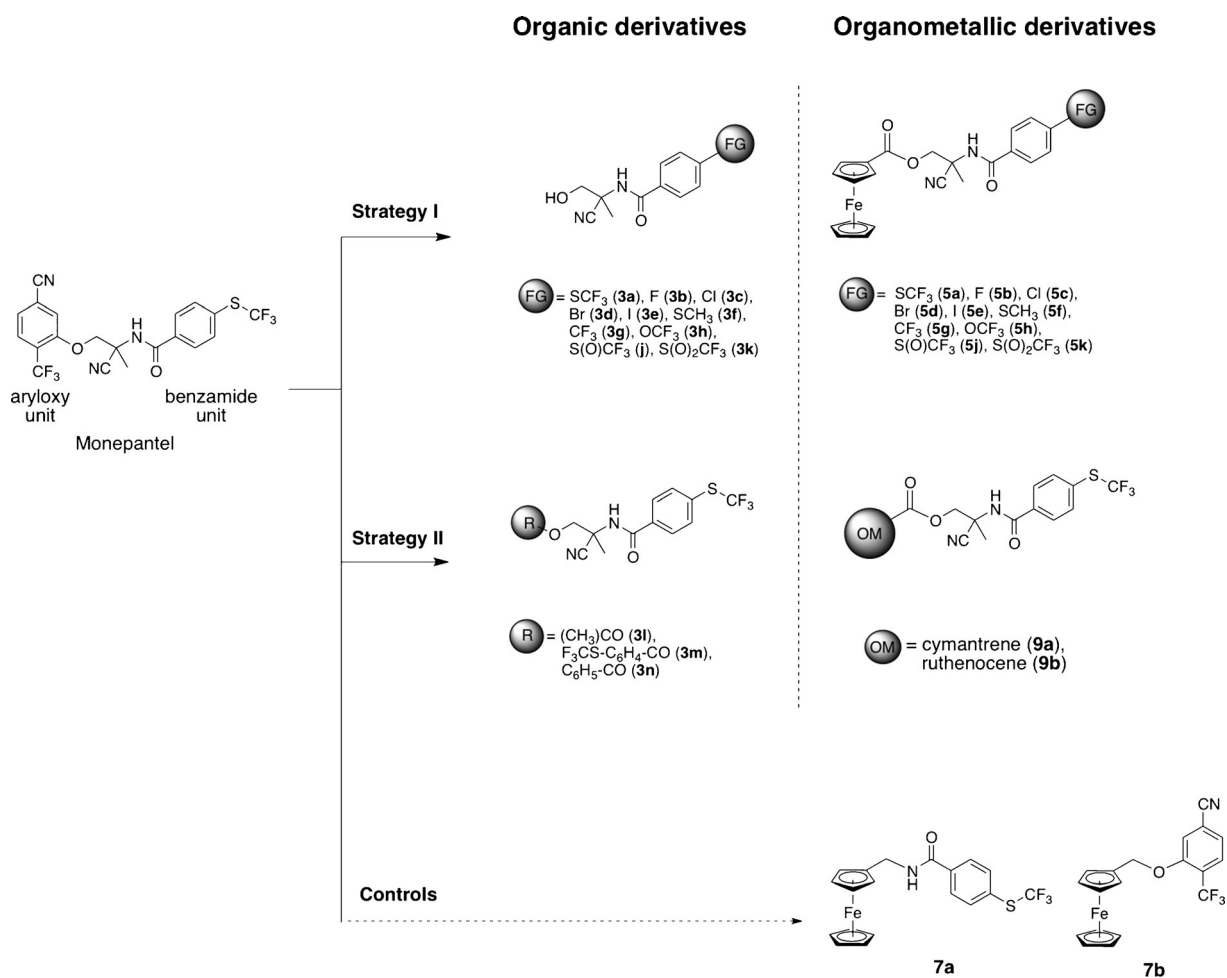
Design of organometallic analogues

Monepantel consists of an aryloxy and a benzamide unit connected by a chiral C₂ spacer. Preliminary metabolism studies indicated that the benzamide unit plays a crucial role in the in

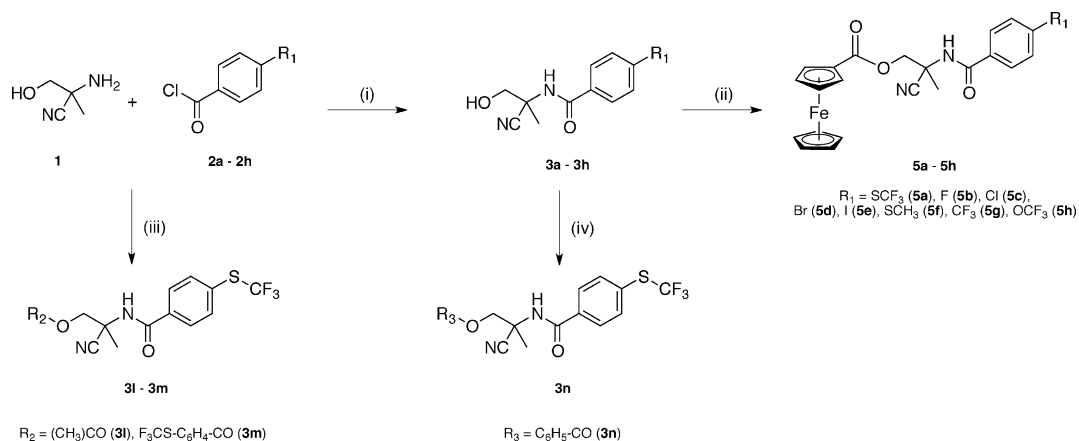
vivo activity of monepantel.^[18] Therefore, with the intention to keep the benzamide part in place, we designed our first organometallic monepantel analogues by replacing the aryloxy part of monepantel with a ferrocenyl unit (Scheme 1). The ferrocene/ferrocenium system has redox properties favorable for production of ROS, which can improve toxicity, as shown for ferroquine and ferrocifen.^[11b,19] Subsequently, we employed two different strategies to study the SAR of monepantel analogues. In Strategy I, a series of organic and organometallic derivatives were synthesized in which the functional group at the 4-position of the benzamide moiety was varied (Scheme 1). In Strategy II (Scheme 1), we designed organic and organometallic derivatives of **5a** in order to evaluate the importance of the organometallic moiety. For this purpose, the ferrocenyl subunit was swapped with two different organometallic moieties, namely, ruthenocene and cymantrene. Replacing the Fe^{II} core with a comparatively inert Ru^{II} center may allow us to probe the relevance of Fe^{II}/Fe^{III}-mediated redox activity of the compound. By contrast to ferrocene and ruthenocene, cymantrene conjugates of organic drugs are rarely studied for their antiparasitic potency.^[20] The metal center in cymantrene is isoelectronic to that of ferrocene and the two metallocenes are nearly isosteric. However, they have different redox behavior, and the metal centers are in +1 and +2 oxidation states in cymantrene and ferrocene, respectively. Therefore, comparison of these metallocenyl analogues should illuminate any metal-mediated modes of action of our compounds.

Synthesis and characterization

Organometallic analogues **5a–5h** were prepared in a two-step procedure as outlined in Scheme 2. The central core, 2-amino-2-hydroxymethylpropionitrile (**1**), was synthesized by following the procedure described by Gauvry et al.^[21] In a subsequent reaction, the amide bond between **1** and the commercially available compounds **2a–2h** bearing a chlorocarbonyl moiety was formed. Initially, we attempted to synthesize **3a** by following the procedure of Gauvry et al.^[21] However, instead of the desired compound, two different products, namely 2-cyano-2-[(trifluoromethyl)thio]benzamido]propyl acetate (**3l**) and 2-cyano-2-[(trifluoromethyl)thio]benzamido]propyl 4-[(trifluoromethyl)thio]benzoate (**3m**) were isolated in yields of 21% and 3%, respectively (Scheme 2). Therefore, we improved the protocol by changing the base from sodium hydroxide to triethylamine, which resulted in the formation of the desired **3a** in 74% yield. By following the same procedure, compounds **3b–3h** were isolated in moderate to good yields. Compound **3a** was further treated with benzoyl chloride under basic conditions, and compound **3n** was obtained in 86% yield. Finally, esterification of **3a–3h** with ferrocenecarboxylic acid (**4**) yielded the desired compounds **5a–5h** as yellow or orange solids. Although it was shown that the efficacy of AADs against nematodes is enantioselective, we decided to perform the synthesis and biological evaluation with the organometallic racemates (**5a–5h**). Lower potency is expected for racemic mixtures rather than enantiopure compounds, but this approach provided an initial estimation of potency.



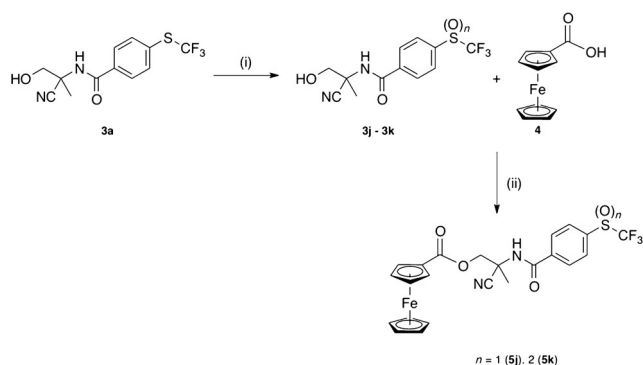
Scheme 1. Schematic representation of the design of organometallic derivatives based on the lead structure of AAD 1566 (monepantel).



Scheme 2. Reagents and conditions: i) NEt_3 , dry CH_2Cl_2 , 1.5 h–24 h, r.t., 26%–74%. ii) a) Ferrocenecarboxylic acid (**4**), oxalyl chloride, dry CH_2Cl_2 , r.t.; b) NEt_3 , dry CH_2Cl_2 , overnight (o.n.), r.t., 25%–94% after two steps. iii) 4-(Trifluoromethylthio)benzoyl chloride, dry ethyl acetate, 1 M NaOH, 3 h, r.t., 21% (**3l**) and 3% (**3m**). iv) Benzoyl chloride, NEt_3 , dry CH_2Cl_2 , 2 h, r.t. 86% (**3n**).

Monepantel is rapidly metabolized *in vivo* to the sulfone derivative, with the corresponding sulfoxide as an intermediate.^[18,22] Because these are active metabolites,^[22] we synthesized the sulfone and sulfoxide derivatives of **5a** (**5j** and **5k**, Scheme 3). For this purpose, the SCF_3 functionality of **3a** was

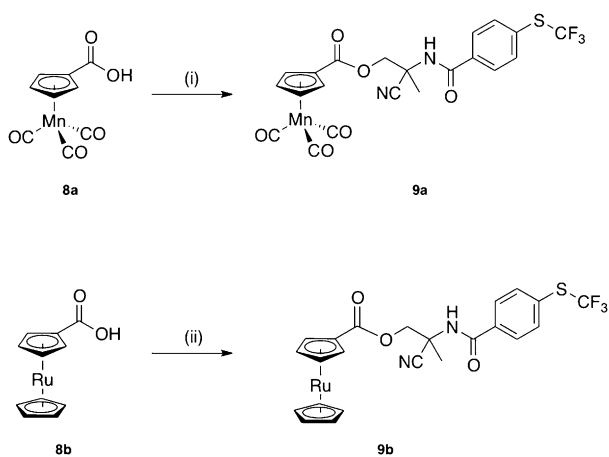
selectively oxidized with different equivalents of *meta*-chloroperoxybenzoic acid (*m*-CPBA) at -78°C . The resulting organic precursors **3j** and **3k** were isolated as colorless solids in moderate yields. Esterification of **3j** or **3k** with **4** yielded the final ferrocenyl-based sulfoxide and sulfone derivatives, 2-cyano-2-



Scheme 3. Reagents and conditions: (i) *m*-CPBA, dry CH_2Cl_2 , $-78^\circ\text{C} \rightarrow \text{r.t.}$, 45% (**3j**) and 43% (**3k**). (ii) a) Oxalyl chloride, dry CH_2Cl_2 , r.t.; b) NEt_3 , dry CH_2Cl_2 , o.n., r.t., 70% (**5j**) and 87% (**5k**) over two steps.

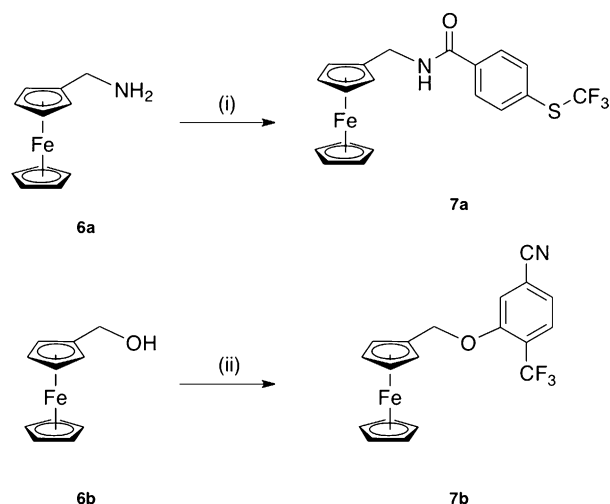
4-[[trifluoromethyl]sulfonyl]benzamido}propyl ferrocenoate (**5j**) and 2-cyano-2-[4-[[trifluoromethyl]sulfonyl]benzamido}propyl ferrocenoate (**5k**, Scheme 3).

The ferrocenyl moiety of **5a** was replaced with two different organometallic moieties to assess their effect on the anthelmintic activity. In contrast to the ferrocenyl derivative **5a**, the cymantrene derivative **9a** and ruthenocene derivative **9b** (Scheme 4) are not expected to produce ROS. Compounds **9a** and **9b** were synthesized by following the synthetic pathway outlined in Scheme 4. Initially, cymantrene carboxylic acid (**8a**) and ruthenocenyl carboxylic acid (**8b**) were synthesized according to published procedures.^[23] Whereas **8a** was linked to **3a** by a one-step Steglich esterification reaction, **8b** required activation with oxalyl chloride and then reaction with **3a**.



Scheme 4. Reagents and conditions: i) **3a**, dicyclohexylcarbodiimide, 4-dimethylaminopyridine, dry $\text{Et}_2\text{O}/\text{CH}_2\text{Cl}_2$, 24 h, $0^\circ\text{C} \rightarrow \text{r.t.}$, 74%. ii) a) Oxalyl chloride, dry CH_2Cl_2 ; b) **3a**, NEt_3 , dry CH_2Cl_2 , r.t., o.n., 41% after two steps.

To assess the importance of the chiral C_2 spacer between the aryloxy and benzamide units, two additional organometallic derivatives were synthesized. Compounds **7a** and **7b** contain benzamide and aryloxy units, respectively, which are connected to a ferrocenyl moiety via an amide or an ether functionality, rather than the C_2 spacer (Scheme 5). The organome-



Scheme 5. Reagents and conditions: i) 4-(Trifluoromethylthio)benzoyl chloride, NEt_3 , dry THF, 16 h, r.t., 32%. ii) 3-Fluoro-4-(trifluoromethyl)benzonitrile, NaH, dry THF, $0^\circ\text{C} \rightarrow \text{r.t.}$, 36 h, 16%.

tallic precursors ferrocenylmethylamine (**6a**) and hydroxymethylferrocene (**6b**) were synthesized following published procedures.^[24] Compound **7a** was then readily prepared by amide bond formation of **6a** with commercially available 4-(trifluoromethylthio)benzoyl chloride under alkaline conditions and *N*-ferrocenyl-4-(trifluoromethylthio)benzamide (**7a**) was isolated as a bright yellow solid. 3-(Ferrocenyloxy)-4-(trifluoromethyl)benzonitrile (**7b**) was isolated after an aromatic nucleophilic substitution reaction with the ferrocenyl alcohol (Scheme 5).

All new compounds were unambiguously characterized by ^1H , ^{13}C , and ^{19}F NMR spectroscopy, mass spectrometry, and IR spectroscopy, and their purities were verified by elemental analysis (see Experimental Section and Supporting Information for further details). The ^{13}C NMR spectra of the compounds containing a fluorine atom (**3a**, **3b**, **3g**, **3h**, **3j**, **3k**, **3l**, **3m**, **3n**, **5a**, **5b**, **5g**, **5h**, **5j**, **5k**, **7a**, **7b**, **9a**, and **9b**) showed a characteristic coupling to the adjacent carbon atom resulting in a quadruplet splitting pattern. Most of the derivatives were detected mainly as their $[M+H]^+$ species by ESI mass spectrometry (positive detection mode) with traces of $[M+Na]^+$ and $[M+K]^+$ species present.

X-ray crystallography

The structures of compounds **3a**, **3b**, **3f**, **3g**, **5a**, **5c**, **5d**, **5h**, and **5k** were further corroborated by single-crystal X-ray diffraction studies. Example structures of **3f** and **5d** are shown in Figure 2 (see Figure S1–S3 in the Supporting Information for the other structures). The X-ray diffraction studies confirmed the formation of the amide bond between the 2-amino-2-hydroxymethylpropionitrile species **1** and the substituted compounds **2a–2h** through the carbonyl group to form the monopantel analogues. The reported crystal structure of monopantel contains four crystallographically independent molecules of the *S* enantiomer, which only differ from each other in the ori-

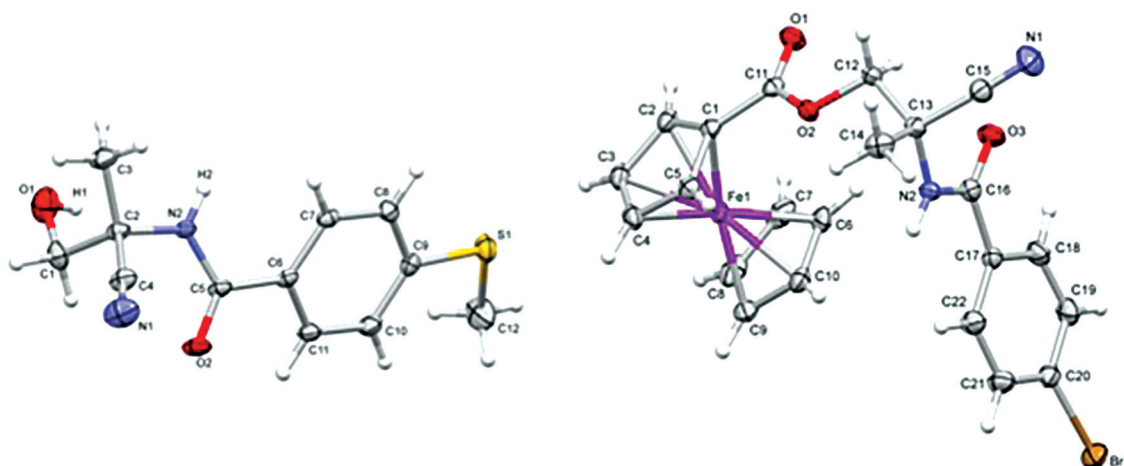


Figure 2. Molecular structure of compounds **3 f** (left) and **5 d** (right) with atomic numbering schemes.

entation of the terminal SCF_3 group relative to the rest of the molecule.^[5] The central part of the monepantel enantiomer exhibits a *Z*-type conformation between the chiral carbon atom C^* and the carbonyl oxygen atom (on the same side of the central $\text{C}-\text{N}$ bond), together with an *E*-type conformation between the carbonyl carbon atom and the methyl group (on opposite sides of the $\text{N}-\text{C}^*$ bond) along the $(\text{O}=\text{C})-\text{N}(\text{H})-\text{C}^*-\text{CH}_3$ moiety. Indeed, the $\text{O}-\text{C}-\text{N}-\text{C}^*$ torsion angles in the independent molecules are close to 0° (*Z*-type), between $1.9(5)$ and $5.7(5)^\circ$. This very narrow range was expected because of the pronounced double-bond character of the central bond, due to electron delocalization with the carbonyl group (as revealed by relatively short $\text{C}-\text{N}$ bond lengths in the range $1.355(4)$ – $66(5)$ Å). Despite the single-bond character of the $\text{N}-\text{C}^*$ bond ($1.452(6)$ – $62(5)$ Å), the $\text{C}-\text{N}-\text{C}^*-\text{C}$ torsion angles also lie in a narrow range close to 180° (*E*-type; $165.4(4)$ – $169.0(4)^\circ$).

The *Z*-type conformation is observed in all our new aminoacetonitrile derivatives. The largest $\text{O}-\text{C}-\text{N}-\text{C}^*$ torsion angle was found in the crystal structure of **3 a** with a value as small as $8.6(2)^\circ$. More interestingly, the *E*-type conformation is also generally observed in our compounds: all $\text{C}-\text{N}-\text{C}^*-\text{C}$ torsion angles lie in the range $160.4(3)$ – $179.0(1)^\circ$, except for **3 a** with $72.9(2)$, $62.0(2)^\circ$ and **5 k** with $59(2)/68.0(6)^\circ$ (two-component disorder). The crystal structures of **5 c**, **5 d**, **5 f**, **5 g**, and **5 k** confirmed coordination of the organic species on a ferrocenyl moiety to form a carboxyl group. The CO_2 fragment is essentially coplanar with the five-membered ring, and the $\text{C}-\text{C}$ bond between the ring and the carboxyl group lies in the normal range for a $\text{C}(\text{sp}^2)-\text{C}(\text{sp}^2)$ single bond (from $1.459(2)$ Å for **5 k** to $1.484(6)$ Å for **5 f**). The relative orientation of the rest of the molecule with the ferrocenyl moiety mainly depends on the intermolecular interactions that link the molecules in the solid state, mainly $\text{C}-\text{H}\cdots\text{O}$, $\text{C}-\text{H}\cdots\text{N}$, and $\text{N}-\text{H}\cdots\text{O}$ hydrogen bonds, as observed in the crystal structures of the organic molecules **3 a**, **3 b**, **3 f**, and **3 g**. All compounds except **3 g** crystallized in triclinic, monoclinic, or orthorhombic centrosymmetric space groups, which indicates the presence of both *R* and *S* enantiomers (racemates) in the crystals. Compound **3 g** crystallized in a racemic crystal structure as well, but in the noncentrosym-

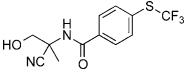
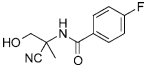
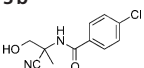
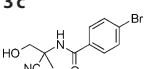
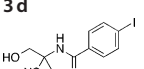
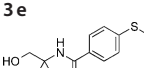
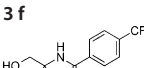
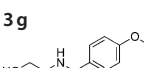
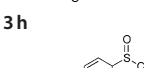
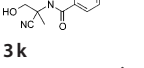
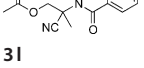
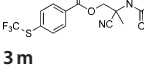
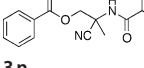
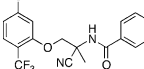
metric space group *Pna2*₁, with two crystallographically independent *S* and *R* enantiomer molecules in the asymmetric unit in a 1:1 ratio.

Activity against *H. contortus* and *Trichostrongylus colubriformis*

H. contortus and *T. colubriformis* are common parasitic nematodes of ruminants and are responsible for major economic losses on farms worldwide.^[1e] *H. contortus* is located in the abomasum (stomach) of the host, where it feeds on blood, whereas *T. colubriformis* affects the anterior small intestine.^[1e] Since these species can coexist in similar climatic regions and co-infect animals, it is desirable to have anthelmintics that efficiently kill both parasites.^[1e] Here, all organic precursors and organometallic analogues of monepantel were screened for their activities against these two parasites in a larval development assay (LDA, see Supporting Information for details), and the results are summarized in Tables 1 and 2.

At the highest concentration tested ($10 \mu\text{g mL}^{-1}$), nine of the 27 compounds showed moderate activities against *H. contortus* and *T. colubriformis*, with EC_{60} values ranging from 1.80 to $9.50 \mu\text{g mL}^{-1}$ (3.30 – $31.20 \mu\text{M}$). The potencies of our compounds were lower than that of the parent compound monepantel against *H. contortus* and *T. colubriformis*.^[5] Most of the organic intermediates **3 a**–**3 k** were not active. However, the insertion of the ferrocenyl moiety generally increased activity, as observed for compounds **5 a**, **5 e**, **5 h**, and **5 k**. Specifically, **3 a**, the organic precursor of **5 a**, had EC_{60} values of $9.50 \mu\text{g mL}^{-1}$ ($31.20 \mu\text{M}$) and $>10.00 \mu\text{g mL}^{-1}$ ($>32.90 \mu\text{M}$) against *H. contortus* and *T. colubriformis*, respectively; by contrast, **5 a** showed EC_{60} values of $2.10 \mu\text{g mL}^{-1}$ ($4.07 \mu\text{M}$) and $6.30 \mu\text{g mL}^{-1}$ ($12.20 \mu\text{M}$), respectively. Within the series of halide-containing organometallic compounds (**5 b**–**5 e**), **5 e**, with an iodo substituent, showed an EC_{60} of $4.5 \mu\text{g mL}^{-1}$ ($8.30 \mu\text{M}$) against *H. contortus*. However, this compound was inactive ($>10 \mu\text{g mL}^{-1}$ / $>18.45 \mu\text{M}$) against *T. colubriformis*; **5 e** was the only analogue shown to be active against *H. contortus* but not against *T. colubriformis*.

Table 1. Activity of organic intermediates **3a–3n** against *Haemonchus contortus* and *Trichostrongylus colubriformis* in an LDA and against *Dirofilaria immitis* microfilariae in vitro. The experiments were performed in two series of triplicate dose responses leading to six individual measurements. EC values were calculated from the means of these individual measurements. The experimental errors are not reported, as they are considered too low to influence the overall EC values.

Compound	EC ₆₀ value				EC ₅₀ value			
	<i>H. contortus</i> [μg mL ⁻¹]	[μM]	<i>T. colubriformis</i> [μg mL ⁻¹]	[μM]	<i>D. immitis</i> , 24 h [μg mL ⁻¹]	[μM]	<i>D. immitis</i> , 48 h [μg mL ⁻¹]	[μM]
 3a	9.50	31.20	> 10.00	> 32.90	> 10.00	> 32.90	0.49	1.61
 3b	> 10.00	> 45.00	> 10.00	> 45.00	> 10.00	> 45.00	> 10.00	> 45.00
 3c	> 10.00	> 41.90	> 10.00	> 41.90	> 10.00	> 41.90	6.60	27.65
 3d	> 10.00	> 35.32	> 10.00	> 35.32	> 10.00	> 35.32	> 10.00	> 35.32
 3e	> 10.00	> 30.29	> 10.00	> 30.29	> 10.00	> 30.29	> 10.00	> 30.29
 3f	> 10.00	> 39.94	> 10.00	> 39.94	> 10.00	> 39.94	> 10.00	> 39.94
 3g	> 10.00	> 36.73	> 10.00	> 36.73	> 10.00	> 36.73	> 10.00	> 36.73
 3h	> 10.00	> 34.70	6.60	22.89	> 10.00	> 34.70	> 10.00	> 34.70
 3j	> 10.00	> 31.22	> 10.00	> 31.22	> 10.00	> 31.22	6.60	20.61
 3k	> 10.00	> 29.74	> 10.00	> 29.74	> 10.00	> 29.74	> 10.00	> 29.74
 3l	3.00	8.66	4.00	11.55	> 10.00	> 28.88	6.60	19.06
 3m	> 10.00	> 19.67	> 10.00	> 19.67	> 10.00	> 19.67	6.60	12.98
 3n	4.20	10.28	5.80	14.20	> 10.00	> 24.49	> 10.00	> 24.49
 AA 85	0.01 ^[a]	0.022 ^[a]	0.032 ^[a]	0.07 ^[a]	2.40	5.25	2.20	4.81
 AA 96	0.01 ^[a]	0.021 ^[a]	0.032 ^[a]	0.07 ^[a]	n.d.i. ^[b]	n.d.i.	n.d.i.	n.d.i.
ivermectin	0.001 ^[a]	0.001 ^[a]	0.01 ^[a]	0.001 ^[a]	1.00–3.00	1.14–3.43	1.00–3.00	1.14–3.43

[a] EC₁₀₀ value.^[5] [b] n.d.i. = non-disclosable information.^[25]

Table 2. Activity of organometallic analogues of monepantel **5a–5h**, **7a**, **7b**, **9a** and **9b** against *Haemonchus contortus* and *Trichostrongylus colubriformis* in an LDA and against *Dirofilaria immitis* microfilariae in vitro. The experiments were performed in two series of triplicate dose responses leading to six individual measurements. EC values were calculated from the means of these individual measurements. The experimental errors are not reported, as they are considered too low to influence the overall EC values.

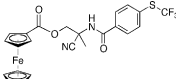
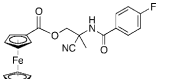
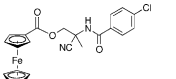
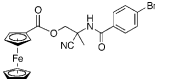
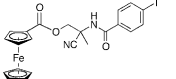
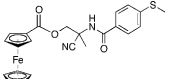
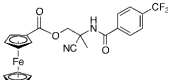
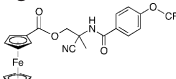
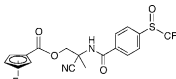
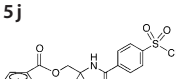
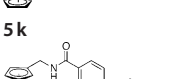
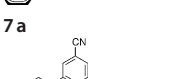
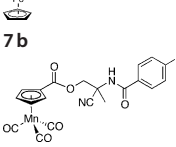
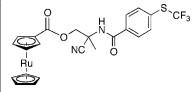
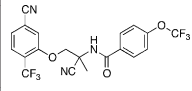
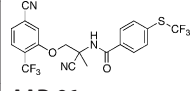
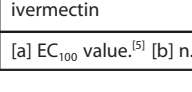
Compound	EC ₆₀ value				EC ₅₀ value			
	<i>H. contortus</i> [μg mL ⁻¹]	[μM]	<i>T. colubriformis</i> [μg mL ⁻¹]	[μM]	<i>D. immitis</i> , 24 h [μg mL ⁻¹]	[μM]	<i>D. immitis</i> , 48 h [μg mL ⁻¹]	[μM]
 5a	2.10	4.07	6.30	12.20	> 10.00	> 19.37	> 10.00	> 19.37
 5b	> 10.00	> 23.03	> 10.00	> 23.03	> 10.00	> 23.03	6.60	15.20
 5c	> 10.00	> 22.19	> 10.00	> 22.19	> 10.00	> 22.19	6.60	14.64
 5d	> 10.00	> 20.20	> 10.00	> 20.20	> 10.00	> 20.20	4.20	8.48
 5e	4.50	8.30	> 10.00	> 18.45	> 10.00	> 18.45	6.60	12.17
 5f	> 10.00	> 21.63	> 10.00	> 21.63	> 10.00	> 21.63	> 10.00	> 21.63
 5g	> 10.00	> 20.65	> 10.00	> 20.65	> 10.00	> 20.65	6.60	13.63
 5h	3.00	6.00	7.00	14.00	> 10.00	> 20.00	> 10.00	> 20.00
 5j	> 10.00	> 18.79	> 10.00	> 18.79	> 10.00	> 18.79	> 10.00	> 18.79
 5k	1.80	3.30	4.60	8.40	> 10.00	> 18.24	> 10.00	> 18.24
 7a	6.00	14.31	8.30	19.79	2.00	5.25	2.10	5.10
 7b	> 10.00	> 26.00	> 10.00	> 26.00	> 10.00	> 26.00	> 10.00	> 26.00
 9a	> 10.00	> 18.71	> 10.00	> 18.71	> 10.00	> 18.71	1.80	3.37

Table 2. (Continued)

Compound	EC ₆₀ value				EC ₅₀ value			
	<i>H. contortus</i> [μg mL ⁻¹]	[μM]	<i>T. colubriformis</i> [μg mL ⁻¹]	[μM]	<i>D. immitis</i> , 24 h [μg mL ⁻¹]	[μM]	<i>D. immitis</i> , 48 h [μg mL ⁻¹]	[μM]
 9a	> 10.00	> 17.80	> 10.00	> 17.80	> 10.00	> 17.80	> 10.00	> 17.8
 9b	0.01 ^[a]	0.022 ^[a]	0.032 ^[a]	0.07 ^[a]	2.40	5.25	2.20	4.81
 AAAD 85	0.01 ^[a]	0.021 ^[a]	0.032 ^[a]	0.07 ^[a]	n.d.i. ^[b]	n.d.i.	n.d.i.	n.d.i.
 AAAD 96	0.001 ^[a]	0.001 ^[a]	0.01 ^[a]	0.01 ^[a]	1.00–3.00	1.14–3.43	1.00–3.00	1.14–3.43

[a] EC₁₀₀ value.^[5] [b] n.d.i. = non-disclosable information.^[25]

Exchange of the SCF₃ group in **5a** with an OCF₃ group in **5h** led to a slight decrease in activity against both parasites (EC₆₀ increased by 43% for *H. contortus* and by 11% for *T. colubriformis*). Oxidizing the SCF₃ group of **5a** to its sulfone in **5k** increased the activity slightly (EC₆₀ decrease of 14% for *H. contortus* and 27% for *T. colubriformis*). However, the sulfoxide **5j** had no activity at the highest concentration tested (> 10 μg mL⁻¹, > 18.79 μM). Overall, the order of potencies for substituents at the benzamide unit of the active analogues of **5a** is S(O)₂CF₃ ≥ SCF₃ ≥ OCF₃ > I.

Replacement of the ferrocenyl moiety of **5a** with a cymantrenyl and ruthenocenyl unit in **9a** and **9b**, respectively, rendered the compound inactive against *H. contortus* and *T. colubriformis*. The inactivity of **9b**, in particular, suggests that **5a** may have a partial metal-coupled mode of action. Based on previous biological studies on ferrocenyl and ruthenocenyl derivatives,^[11b, 16b, 19a, 26] it seems reasonable to speculate that the ferrocene moiety of **5a**, but not the ruthenocene moiety in **9b**, can cause ROS generation inside the parasite, and that this ROS is at least partly responsible for the activity of **5a**. Indeed, we found that ROS generation by **5a** is significantly higher than that of **9b**, as described below.

Potentiation of ion-channel current

The ferrocenyl compound **5a** was more efficacious against *H. contortus* and *T. colubriformis* than its organic counterpart **3a**. This difference may arise from the ability of the ferrocenyl compound to potentiate the ion channels better than the organic counterpart. Alternatively, the presence of the hydrophobic ferrocenyl entity in **5a** might enhance the accumulation of the compound in the worm's tissues, or impart a secondary function, such as ROS production. To test whether better potentiation of ion channel currents contributed to the increased efficacy of **5a**, we compared the ability of compounds **3a**, **3l**, and **5a** to potentiate the monepantel target ACR-23 of *C. ele-*

gans expressed in oocytes of *Xenopus laevis*. Monepantel acts as a positive allosteric modulator, increasing ion channel current when it is co-applied with an agonist.^[6a, c, 7] To quantify the potentiation of this channel by our compounds, we co-applied them with the agonist betaine (300 μM, ≈ EC₁₀) and compared the current with control recordings for betaine alone.

All three compounds showed decent efficacies in this assay. The least potent and efficacious compound was **3l**, with an EC₅₀ of 9 μM and maximal potentiation of ninefold compared with the current induced by betaine alone. The potency and efficacy of compounds **3a** and **5a** were similar; **3a** had an EC₅₀ of 2.1 μM, with maximal potentiation of 30-fold, and **5a** had an EC₅₀ of 1.2 μM, with maximal potentiation of 32-fold (Figure 3). The less than twofold difference in EC₅₀ values between these two compounds is negligible, and seems to result mostly from a considerable difference in the slope of the response curves (Hill coefficient: 2.1 for **3a** and 11.5 for **5a**). The steep slope of the curve for **5a** could be caused by limited aqueous solubility affecting the measurements at higher concentrations.

The efficacy of these three compounds potentiating ACR-23 channels follows the order **5a** ≈ **3a** > **3l**. This efficacy differs from that against *H. contortus* and *T. colubriformis*, which follows the order **5a** ≈ **3l** > **3a**. The marked efficacy of **3a** when assayed on the ion channel demonstrates that the ferrocenyl group of **5a** and the corresponding aryloxy group of monepantel are not essential for receptor potentiation. Therefore, the aryloxy group of monepantel is likely to contribute to favorable pharmacokinetic properties or pharmacological potency, rather than efficacy. The ferrocenyl group of **5a** either partially recapitulates these properties, or confers novel toxic properties. These results are consistent with the differences in antiparasitic activity of compounds **5a** and **9b**, and indicate that redox-mediated toxic properties of ferrocene may contribute to the toxicity of **5a**.

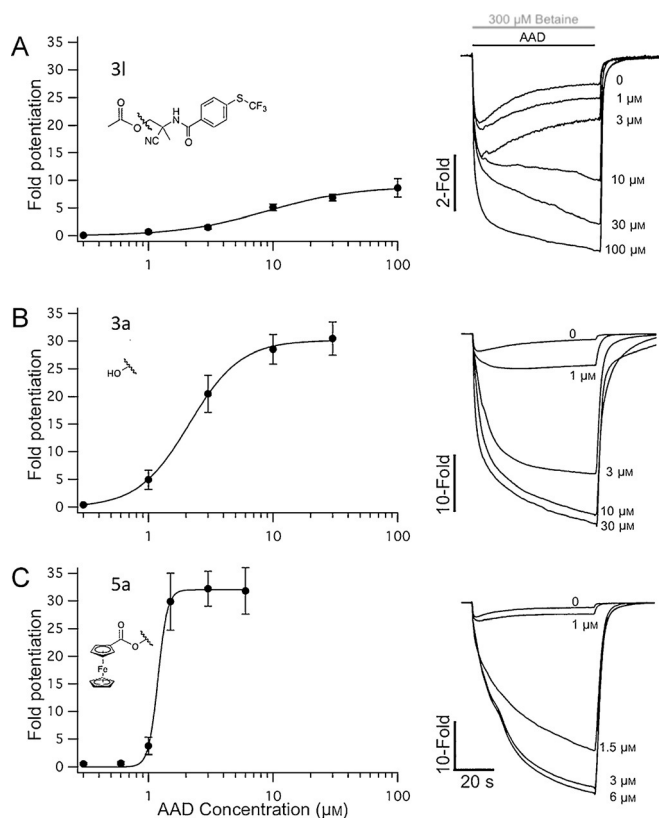


Figure 3. Potentiation of ACR-23 channels expressed in *Xenopus laevis* oocytes. A) Compound **3I**. B) Compound **3a**. C) Compound **5a**. Left: concentration-response curves. Insets indicate the chemical groups that are different between the three compounds. *x*-Fold potentiation represents the current after 1 min of sustained co-application with betaine (300 μM), normalized to the current from applying betaine alone. $n=5-8$ recordings from independent oocytes. Error bars are standard errors of the mean. Right: representative current traces from co-application of AAD compounds with the agonist betaine.

Production of ROS

The rationale behind the design of our organometallic-containing monepantel derivatives was the introduction of metal-specific modes of action into the organic drug. For example, we envisaged that the redox properties of the ferrocene/ferrocenium system in **5a** might lead to the production of toxic ROS and thus improve antiparasitic activity of the organic drug.^[27] As discussed earlier, **5a** exhibited moderate activity against *H. contortus* and *T. colubriformis*, but ruthenocenyl analogue **9b** is inactive. To confirm that our compounds have the predicted redox properties, we assessed ROS induced by selected compounds (**3a**, **5a**, **9a**, and **9b**) in living cells. Although it would have been ideal to investigate ROS production in parasites, for practical and technical reasons, we used a mammalian cervical cancer cell line (HeLa). To this end, cells were treated with different compounds (25 μM for 20 h), and the intracellular ROS was quantified with the oxidation-sensitive fluorescent indicator 2',7'-dichlorofluorescein diacetate (H2DCFDA); *tert*-butyl hydroperoxide (TBH) was employed as a positive control (100 μM for 6 h). The ROS level in cells treated with **3a** was similar to that of the untreated control cells. By contrast, compound **5a**,

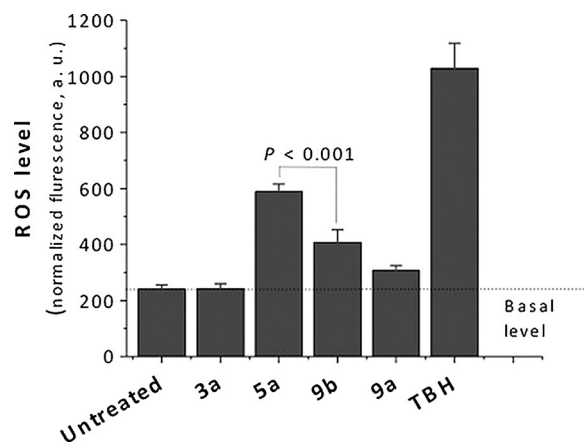


Figure 4. Level of ROS in HeLa cells treated with **3a**, **5a**, **9a** and **9b**. TBH: *tert*-butyl hydroperoxide.

which results from the attachment of a ferrocenyl moiety to **3a**, produced a 2.4-fold higher level of ROS than organic precursor **3a** alone. ROS induced by the ruthenocene analogue **9b** was significantly ($P < 0.001$) lower than for **5a**. This difference in ROS production might be one of the factors responsible for the difference in potency between **5a** and **9b** against *H. contortus* and *T. colubriformis* (Figure 4). Additionally, we evaluated ROS production following exposure to the cyanotrene analogue **9a**. The ROS level induced by **9a** was comparable to its organic precursor (**3a**).

Activity against filarial nematodes

As organometallic derivatization was shown previously to modulate the activity profiles of organic drugs,^[11b, 16b, 26] we assayed the activity of our new class of anthelmintics against other parasites. We were eager to assess the activity of our compounds on taxonomically and biologically disparate groups of parasites, including *D. immitis* (canine heartworm), *Ctenocephalides felis* (cat flea), *Lucilia cuprina* (blow fly), and *Rhipicephalus sanguineus* (brown dog tick). Neither AAD 85 nor the compounds synthesized in this study had activity (at the highest concentration tested) on *C. felis* (100 $\mu\text{g mL}^{-1}$), *L. cuprina* (32 $\mu\text{g mL}^{-1}$), or *R. sanguineus* (100 $\mu\text{g mL}^{-1}$ and 640 $\mu\text{g mL}^{-1}$) (Supporting Information, Table S4). Compound **5a** and four other compounds effective against *H. contortus* and *T. colubriformis* in an LDA (**3h**, **3n**, **5h**, and **5k**) exhibited no activity against *D. immitis* in a motility assay. However, 12 out of 27 compounds showed considerable activity against *D. immitis* microfilariae, in a similar range to that of the standard anti-heartworm agent ivermectin.^[28] The organic precursor **3a** was extremely active against this parasite, with an EC_{50} value of 0.49 $\mu\text{g mL}^{-1}$ (1.61 μM) after 48 h. Other organic precursors (**3c**, **3j**, **3l**, and **3m**) had lower activities, with EC_{50} values of 6.60 $\mu\text{g mL}^{-1}$ (12.98–27.65 μM). The activities of organometallic derivatives were moderate; **5b**, **5c**, **5d**, **5e**, **5g**, and **7a** showed EC_{50} values of 2.00–6.60 $\mu\text{g mL}^{-1}$ (5.10–15.20 μM). Interestingly, the organometallic analogue **7a**, bearing only the benzamide unit and lacking the C_2 spacer, was the only com-

pound that was active against all three parasitic nematodes tested (i.e., *H. contortus*, *T. colubriformis*, and *D. immitis*); **7a** is also the only compound that displayed activity after only 24 h. The replacement of ferrocene in **5a** with a cymantrene unit makes the resultant analogue **9a** active against *D. immitis*, with an EC₅₀ value of 1.80 μg mL⁻¹ (3.37 μM).

Because AAD activity against filarial nematodes has not been reported previously, we decided to also test a close analogue of monepantel, namely, AAD 85. This compound has activity similar to that of **7a**; it is less potent than **3a**, but acts within 24 h. The *D. immitis* genome does not appear to encode a close homologue of the receptors targeted by monepantel, which suggests that this species has a novel AAD target. Moreover, the lack of a correlation between ROS production and activity against *D. immitis* indicates that the activity against *D. immitis* is not specifically caused by ROS.

Cytotoxicity and stability of **3a** and **9a**

An ideal antiparasitic compound would be selective in killing worms while being nontoxic to the mammalian host. We evaluated the selectivity of the two most active compounds against *D. immitis*, **3a** and **9a**. We determined their cytotoxicity using noncancerous human embryonic kidney (HEK293) cells. The metal-based anticancer drug cisplatin was used as positive control. Cisplatin inhibits the growth of HEK293 cells with an IC₅₀ value of 39.62 ± 2.61 μM. Encouragingly, both of the compounds **3a** and **9a** were nontoxic up to 100 μM (the highest concentration assayed), and this demonstrates selectivity of the compounds towards parasites.

Another important parameter is the stability of the drug candidates. The stabilities of **3a** and **9a** were evaluated by ¹H NMR spectroscopy. The compounds were dissolved in [D₆]DMSO/D₂O [1/4 (**3a**), 2/3 (**9a**), v/v] and the solutions kept in the dark at room temperature. ¹H NMR spectra were recorded at different time intervals. No decomposition of the compounds was observed after a 48 h incubation time, and this confirms the stability of **3a** and **9a** in aqueous media (see Figure S4 and S5 of the Supporting Information).

Conclusion

Given the emergence of drug resistance in some socioeconomically important parasitic nematodes, new strategies are needed to discover drugs with novel modes of action. In this study, we explored metal-based variants to expand the chemical space for antiparasitic drug candidates. Starting from the organic drug monepantel as a lead structure, we designed and synthesized a series of organic and organometallic analogues by employing two different strategies. The efficacies of the structurally diverse organometallic analogues as well as various organic intermediates were evaluated against *H. contortus* and *T. colubriformis*. Compounds **3a**, **3h**, **3l**, **3n**, **5a**, **5e**, **5h**, **5k**, and **7a** showed moderate activity against these two nematodes. Further biological assessments on other parasites revealed that 12 of our new compounds had activity against *D. immitis* microfilariae in the low μg mL⁻¹ range of activity for three com-

pounds (**3a**, **7a** and **9a**). Among these three most active compounds, **7a** is a unique candidate showing activity against all three parasitic nematodes. The SAR of compounds active against *H. contortus* and *T. colubriformis* was distinct from the SAR of compounds active against *D. immitis*. This suggests a unique mechanism of action for the compounds in the canine heartworm.

Experimental Section

Synthesis and characterization of organic precursors (**3a–3g**, **3j–3n**) and organometallic analogues (**5a–5k**, **7a**, **7b**, **9a**, **9b**) can be found in the Supporting Information.

Acknowledgements

This work was financially supported by the Swiss National Science Foundation (Professorships N° PP00P2_133568 and PP00P2_157545 to G.G.), the University of Zurich (G.G.), the Stiftung für wissenschaftliche Forschung of the University of Zurich (G.G.), the Novartis Jubilee Foundation (G.G.), and the Swiss Government Excellence Scholarship for Postdoctoral Researcher (R. L.). R.B.G.'s research program is supported by the Australian Research Council (ARC), the National Health and Medical Research Council (NHMRC), Melbourne Water Corporation, Yourgene Bioscience, the Alexander von Humboldt Foundation, and The University of Melbourne. E.M.J. is supported by the US National Institutes of Health (NINDS R01-NS034307) and is an Investigator of the Howard Hughes Medical Institute (HHMI). R.B.G. and E.M.J. are grateful recipients of Professorial Humboldt Research Awards. The authors would like to thank Dr. Jacques Bouvier (Novartis Animal Health, St-Aubin, Switzerland) and Dr. Noëlle Gauvry (Novartis Animal Health, Basel, Switzerland) for their help with the biological assays.

Keywords: anthelmintics · bioorganometallic chemistry · drug design · medicinal chemistry · metallocenes

- [1] a) D. Otranto, R. Wall, *Med. Vet. Entomol.* **2008**, *22*, 291–302; b) N. D. Sargison, *Vet. Parasitol.* **2012**, *189*, 79–84; c) R. K. Grencis, *Annu. Rev. Immunol.* **2015**, *33*, 201–225; d) D. Traversa, *Parasit. Vectors* **2012**, *5*, 91–91; e) F. Roeber, A. Jex, R. Gasser, *Parasit. Vectors* **2013**, *6*, 153; f) R. Kaminsky, L. Rufener, J. Bouvier, R. Lizundia, S. Schorderet Weber, H. Sager, *Vet. Parasitol.* **2013**, *195*, 286–291; g) A. R. Sykes, *Anim. Sci.* **1994**, *59*, 155–172.
- [2] a) L. Holden-Dye, R. J. Walker, *Anthelmintic drugs*, The *C.elegans* Research Community ed., WormBook, **2007**; b) C. Epe, R. Kaminsky, *Trends Parasitol.* **2013**, *29*, 129–134; c) B. E. Campbell, M. Tarleton, C. P. Gordon, J. A. Sakoff, J. Gilbert, A. McCluskey, R. B. Gasser, *Bioorg. Med. Chem. Lett.* **2011**, *21*, 3277–3281; d) B. L. Blagburn, M. W. Dryden, *Vet. Clin. North Am. Small Anim. Pract.* **2009**, *39*, 1173–1200.
- [3] a) R. M. Kaplan, A. N. Vidyashankar, *Vet. Parasitol.* **2012**, *186*, 70–78; b) I. A. Sutherland, D. M. Leathwick, *Trends Parasitol.* **2011**, *27*, 176–181; c) A. J. Wolstenholme, I. Fairweather, R. K. Prichard, G. von Samson-Himelstjerna, N. C. Sangster, *Trends Parasitol.* **2004**, *20*, 469–476; d) R. Van den Brom, L. Moll, C. Kappert, P. Vellema, *Vet. Parasitol.* **2015**, *209*, 278–280; e) A. Mederos, Z. Ramos, G. Bancharo, *Parasit. Vectors* **2014**, *7*, 598; f) A. S. Cezar, G. Toscan, G. Camillo, L. A. Sangioni, H. O. Ribas, F. S. F. Vogel, *Vet. Parasitol.* **2010**, *173*, 157–160; g) T. Coles, M. Dryden, *Parasit. Vectors* **2014**, *7*, 8.

- [4] R. Kaminsky, P. Ducray, M. Jung, R. Clover, L. Rufener, J. Bouvier, S. S. Weber, A. Wenger, S. Wieland-Berghausen, T. Goebel, N. Gauvry, F. Pautrat, T. Skripsky, O. Froelich, C. Komoin-Oka, B. Westlund, A. Sluder, P. Maser, *Nature* **2008**, *452*, 176–180.
- [5] P. Ducray, N. Gauvry, F. Pautrat, T. Goebel, J. Fruechtel, Y. Desaulles, S. S. Weber, J. Bouvier, T. Wagner, O. Froelich, R. Kaminsky, *Bioorg. Med. Chem. Lett.* **2008**, *18*, 2935–2938.
- [6] a) L. Rufener, J. Keiser, R. Kaminsky, P. Mäser, D. Nilsson, *PLoS Pathog.* **2010**, *6*, e1001091; b) L. Rufener, N. Bedoni, R. Baur, S. Rey, D. A. Glauser, J. Bouvier, R. Beech, E. Sigel, A. Puoti, *PLoS Pathog.* **2013**, *9*, e1003524; c) A. S. Peden, P. Mac, Y.-J. Fei, C. Castro, G. Jiang, K. J. Murfitt, E. A. Miska, J. L. Griffin, V. Ganapathy, E. M. Jorgensen, *Nat. Neurosci.* **2013**, *16*, 1794–1801.
- [7] R. Baur, R. Beech, E. Sigel, L. Rufener, *Mol. Pharmacol.* **2014**, *87*, 96–102.
- [8] I. Scott, W. E. Pomroy, P. R. Kenyon, G. Smith, B. Adlington, A. Moss, *Vet. Parasitol.* **2013**, *198*, 166–171.
- [9] a) E. Alessio, Wiley-VCH Verlag, Weinheim, **2011**, Bioinorganic Medicinal Chemistry; b) J. C. Dabrowiak, Metals in Medicine, John Wiley & Sons Ltd, Chichester, **2009**; c) M. Patra, G. Gasser, *ChemBioChem* **2012**, *13*, 1232–1252.
- [10] a) N. J. Farrer, P. J. Sadler, in Bioinorganic Medicinal Chemistry, Wiley-VCH Verlag GmbH & Co. KGaA, **2011**, pp. 1–47; b) P. C. A. Buijinx, P. J. Sadler, *Curr. Opin. Chem. Biol.* **2008**, *12*, 197–206; c) C. G. Hartinger, N. Metzler-Nolte, P. J. Dyson, *Organometallics* **2012**, *31*, 5677–5685.
- [11] a) C. Biot, G. Glorian, L. A. Maciejewski, J. S. Brocard, O. Domaric, G. Blampain, P. Millet, A. J. Georges, H. Abessolo, D. Dive, J. Lebib, *J. Med. Chem.* **1997**, *40*, 3715–3718; b) F. Dubar, T. J. Egan, B. Pradines, D. Kuter, K. K. Ncozazi, D. Forge, J.-F. o. Paul, C. Pierrot, H. Kalamou, J. Khalife, E. Buisine, C. Rogier, H. Vezin, I. Forfar, C. Slomianny, X. Trivelli, S. Kapishnikov, L. Leiserowitz, D. Dive, C. Biot, *ACS Chem. Biol.* **2011**, *6*, 275–287.
- [12] a) R. A. Sanchez-Delgado, A. Anzellotti, *Mini-Rev. Med. Chem.* **2004**, *4*, 23–30; b) A. Martínez, T. Carreon, E. Iniguez, A. Anzellotti, A. Sanchez, M. Tyan, A. Sattler, L. Herrera, R. A. Maldonado, R. A. Sanchez-Delgado, *J. Med. Chem.* **2012**, *55*, 3867–3877; c) L. Otero, G. Aguirre, L. Boiani, A. Denicola, C. Rigol, C. Olea-Azar, J. D. Maya, A. Morello, M. González, D. Gambino, H. Cerecetto, *Eur. J. Med. Chem.* **2006**, *41*, 1231–1239; d) C. R. Maldonado, C. Marin, F. Olmo, O. Huertas, M. Quiros, M. Sanchez-Moreno, M. J. Rosales, J. M. Salas, *J. Med. Chem.* **2010**, *53*, 6964–6972; e) M. Navarro, E. J. Cisneros-Fajardo, T. Lehmann, R. A. Sanchez-Delgado, R. Atencio, P. Silva, R. Lira, J. A. Urbina, *Inorg. Chem.* **2001**, *40*, 6879–6884; f) R. A. Sánchez-Delgado, M. Navarro, K. Lazard, R. Atencio, M. Capparelli, F. Vargas, J. A. Urbina, A. Bouillez, A. F. Noels, D. Masi, *Inorg. Chim. Acta* **1998**, *275–276*, 528–540; g) R. A. Sánchez-Delgado, K. Lazard, L. Rincon, J. A. Urbina, A. J. Hubert, A. N. Noels, *J. Med. Chem.* **1993**, *36*, 2041–2043; h) M. Navarro, T. Lehmann, E. J. Cisneros-Fajardo, A. Fuentes, R. A. Sanchez-Delgado, P. Silva, J. A. Urbina, *Polyhedron* **2000**, *19*, 2319–2325; i) J. J. N. Silva, P. M. M. Guedes, A. Zottis, T. L. Balliano, F. O. Nascimento Silva, L. G. França Lopes, J. Ellena, G. Oliva, A. D. Andricopulo, D. W. Franco, J. S. Silva, *Br. J. Pharmacol.* **2010**, *160*, 260–269; j) E. Iniguez, A. Sanchez, M. Vasquez, A. Martinez, J. Olivias, A. Sattler, R. Sanchez-Delgado, R. Maldonado, *J. Biol. Inorg. Chem.* **2013**, *18*, 779–790; k) M. Navarro, C. Gabbiani, L. Messori, D. Gambino, *Drug Discovery Today* **2010**, *15*, 1070–1078.
- [13] M. Patra, G. Gasser, N. Metzler-Nolte, *Dalton Trans.* **2012**, *41*, 6350–6358.
- [14] a) J. Hess, J. Keiser, G. Gasser, *Future Med. Chem.* **2015**, *7*, 821–830; b) M. Patra, K. Ingram, A. Leonidova, V. Pierroz, S. Ferrari, M. N. Robertson, M. H. Todd, J. Keiser, G. Gasser, *J. Med. Chem.* **2013**, *56*, 9192–9198; c) M. Patra, K. Ingram, V. Pierroz, S. Ferrari, B. Spingler, R. B. Gasser, J. Keiser, G. Gasser, *Chem. Eur. J.* **2013**, *19*, 2232–2235; d) M. Patra, K. Ingram, V. Pierroz, S. Ferrari, B. Spingler, J. Keiser, G. Gasser, *J. Med. Chem.* **2012**, *55*, 8790–8798.
- [15] a) G. Gasser, N. Metzler-Nolte, *Curr. Opin. Chem. Biol.* **2012**, *16*, 84–91; b) G. Gasser, I. Ott, N. Metzler-Nolte, *J. Med. Chem.* **2011**, *54*, 3–25; c) G. Jaouen, N. Metzler-Nolte, in Topics in Organometallic Chemistry, Vol. 32; and references therein, 1st ed., Springer, Heidelberg, Germany, **2010**; d) C. Hartinger, P. J. Dyson, *Chem. Soc. Rev.* **2009**, *38*, 391–401; e) ref. [11]; f) C. Biot, D. Dive, in Medicinal Organometallic Chemistry, Vol. 32 (Eds.: G. Jaouen, N. Metzler-Nolte), Springer, Heidelberg, **2010**, pp. 155–193; g) C. Biot, W. Castro, C. Y. Botte, M. Navarro, *Dalton Trans.* **2012**, *41*, 6335–6349; h) D. Dive, C. Biot, *ChemMedChem* **2008**, *3*, 383–391.
- [16] a) T. Dallagi, M. Saidi, A. Vessières, M. Huché, G. Jaouen, S. Top, *J. Org. Chem.* **2013**, *734*, 69–77; b) G. Jaouen, S. Top, A. Vessières, G. Leclercq, M. J. McGlinchey, *Curr. Med. Chem.* **2004**, *11*, 2505–2517; c) S. Top, A. Vessières, G. Leclercq, J. Quivy, J. Tang, J. Vaissermann, M. Huché, G. Jaouen, *Chem. Eur. J.* **2003**, *9*, 5223–5236.
- [17] P. M. Loiseau, J. J. Jaffe, D. G. Craciunescu, *Int. J. Parasitol.* **1998**, *28*, 1279–1282.
- [18] a) A. Lifschitz, M. Ballent, G. Virkel, J. Sallovitz, P. Viviani, C. Lanusse, *Vet. Parasitol.* **2014**, *203*, 120–126; b) L. Stuchlíková, R. Jirasko, I. Vokral, J. Lamka, M. Spulak, M. Holcapek, B. Szotakova, H. Bartikova, M. Pour, L. Skalova, *Anal. Bioanal. Chem.* **2013**, *405*, 1705–1712.
- [19] a) P. Pigeon, S. Top, A. Vessières, M. Huché, E. A. Hillard, E. Salomon, G. Jaouen, *J. Med. Chem.* **2005**, *48*, 2814–2821; b) N. Chavain, H. Vezin, D. Dive, N. Touati, J.-F. Paul, E. Buisine, C. Biot, *Mol. Pharm.* **2008**, *5*, 710–716.
- [20] a) L. Glans, W. Hu, C. Jost, C. de Kock, P. J. Smith, M. Haukka, H. Bruhn, U. Schatzschneider, E. Nordlander, *Dalton Trans.* **2012**, *41*, 6443–6450; b) P. V. Simpson, C. Nagel, H. Bruhn, U. Schatzschneider, *Organometallics* **2015**, *34*, 3809–3815.
- [21] P. Ducray, N. Gauvry, T. Goebel, M. Jung, R. Kaminsky, F. Pautrat, (Ed.: WO/2005/044784), Google Patents, **2005**.
- [22] D. Karadzovska, W. Seewald, A. Browning, M. Smal, J. Bouvier, J. M. Giraudel, *J. Vet. Pharmacol. Ther.* **2009**, *32*, 359–367.
- [23] a) E. R. Biehl, P. C. Reeves, *Synthesis* **1973**, *1973*, 360–361; b) D. P. Cormode, A. J. Evans, J. J. Davis, P. D. Beer, *Dalton Trans.* **2010**, *39*, 6532–6541.
- [24] a) P. D. Beer, D. K. Smith, *J. Chem. Soc. Dalton Trans.* **1998**, 417–424; b) D. C. G. Hardy, L. Ren, T. C. Tamboue, C. Tang, *J. Polym. Sci. Part A* **2011**, *49*, 1409–1420.
- [25] For legal issues the efficacy of AAD96 cannot be disclosed.
- [26] C. Biot, W. Daher, N. Chavain, T. Fandeur, J. Khalife, D. Dive, E. De Clercq, *J. Med. Chem.* **2006**, *49*, 2845–2849.
- [27] R. Rubbiani, O. Blacque, G. Gasser, *Dalton Trans.* **2016**, *45*, 6619–6626.
- [28] D. D. Bowman, C. Mannella, *Top. Companion Anim. Med.* **2011**, *26*, 160–172.

Received: June 15, 2016
Published online on October 5, 2016